Blending Surface Modelling Using Sixth Order PDEs

L. H. You and Jian J. Zhang
National Centre for Computer Animation
Bournemouth University
United Kingdom

Abstract

In order to model blending surfaces with curvature continuity, in this paper we apply sixth order partial differential equations (PDEs), which are solved with a composite power series based method. The proposed composite power series based approach meets boundary conditions exactly, minimises the errors of the PDEs, and creates almost as accurate blending surfaces as those from the closed form solution that is the most accurate but achievable only for some simple blending problems. Since only a few unknown constants are involved, the proposed method is comparable with the closed form solution in terms of computational efficiency. Moreover, it can be used to construct 3- or 4-sided patches through the satisfaction of continuities along all edges of the patches. Therefore, the developed method is simpler and more efficient than numerical methods, more powerful than the analytical methods, and can be implemented into an effective tool for the generation and manipulation of complex free-form surfaces.

Key Words: curvature continuity surface blending; sixth order partial differential equation; composite power series solution; weighted residual method

1. Introduction

Blending surfaces are widely used in product design. In general, two kinds of blending surfaces are commonly useful: those with tangent and curvature continuities. Although tangent continuity is sufficient for many cases, the ability to satisfy a higher degree of smoothness requirement is essential for various situations. For instance, streamlined surfaces of an automobile are aesthetically appealing and those of an aircraft with curvature continuity can reduce the risk of flow separation and turbulence.

Blending with curvature continuity has been investigated by a number of researchers. Boehm proposed a method to generate curvature continuous curves and surfaces by generalizing the well-known construction of the Bézier points of a cubic spline curve or surface [3]. Jones decomposed an n-sided region into n rectangles and indicated that the rectangular patches are biseptic for curvature continuity [15]. Farin discussed how to construct curvature continuous planar curves consisting of conic segments represented in rational Bézier form [10]. Pegna demonstrated the design of second order smooth blending surfaces by requiring that normal curvatures agree along all tangent directions at the linkage curve of two patches [21]. By sweeping a (possibly variable) circular arc to represent blending surfaces, he gave a method which can guarantee continuity of the unit surface normal and of the normal radius of curvature along the linkage curve [22]. Later on, he and Wolter presented a Linkage Curve theorem that is pertaining to the design of curvature continuous blending surfaces [23]. Zheng et al. investigated the curvature continuity between two adjacent rational Bézier surfaces which may be either rectangular or

triangular [36]. Filkins et al. used an approximation method to blend surfaces which maintain curvature continuity to the underlying surfaces with a non-uniform rational B-spline (NURBS) surface [11]. Schichtel presented a technique for filling polygonal holes using a transfinite interpolant. This technique is to model the second-order smooth transitions at an arbitrary linkage curve between two surfaces [25]. Aumann proposed the so-called normal ringed surfaces to form curvature continuous connections of cones and/or cylinders [1]. Hartmann blended an implicit surface with a parametric surface and achieved G^2-continuous transitions through introduction of a simple additional condition [12]. In his later work, he introduced a method for curvature-continuous (G^2) interpolation of an arbitrary sequence of points on a surface (implicit or parametric) which can be used for G^2 blending of curves on surfaces [13]. Recently, Hartmann proposed the implicit G^n vertex blending methods which can be applied to other surfaces such as parametrically defined surfaces [14]. By defining curvature continuous splines based on 3-sided patches, Peters discussed how to construct smooth surfaces over irregular meshes [24]. Ye developed the Gaussian and mean curvature criteria which individually guarantee the curvature continuity along the linkage curve [27]. He also introduced a method for local construction of a curvature continuous (GC^2) piecewise polynomial surface through the interpolation of a given rectangular curvature continuous quintic curve mesh [28]. Bohl and Reif discussed conditions how degenerate triangular Bézier patches guarantee curvature continuity [4]. Kim et al. demonstrated how to extend a given surface with a piecewise smooth boundary and indicated the extended surface is C^2-continuity along the old boundary [16].

Blending surfaces can also be created using the solutions to PDEs, which has attracted an increasing amount of research efforts. Compared with other more mainstream approaches, this group of techniques prove very flexible in dealing with certain unusual blending problems in addition to the 'ordinary' ones. For example, it can easily blend an open surface with a closed one (Fig. 6) and can also blend surfaces with creases. This would otherwise be extremely challenging for other techniques.

PDE surface generation is a relatively new research topic in geometric modelling, however has already shown a great deal of potential. Bloor and Wilson investigated free-form surface generation with partial differential equations [2]. Lowe et al. created blending surfaces that satisfy certain given design conditions [18]. Dekanski et al. applied PDE method in generation of a properller blade geometry [7]. Du and Qin developed a technique for direct manipulation and interactive sculpting based on PDE and equation of motion [8]. They also considered geometric and physical constraints in dynamic PDE-based surface design [9]. Mimis et al. discussed shape parameterization of a two-stroke engine and optimization of scavenging properties of the engine [19]. Zhang and You applied PDE based approach in vase design [33] and surface blending [34]. Ugail and Wilson combined shape parametrisation with a standard method of numerical optimization and demonstrated the capability of setting up automatic design optimisation problems [26]. You and Zhang extended PDE surface modelling from static problems to dynamic ones [31]. Monterde and Ugail proposed a general PDE method to create Bézier surfaces from the boundary information [20]. These papers and many others employed a fourth order partial differential equation.

Since the vector-valued parameter has a strong influence on the shape of the blending surfaces to be generated, an improved fourth order PDE was proposed by You and Zhang [29]. In this new PDE, three vector-valued parameters were introduced aiming to provide the designer with more control and flexibility on the created blending surfaces. However, these PDEs can only ensure the functional and tangential continuities at the linkage curves, i.e. the highest continuity is C^1. This is because a fourth order PDE will not have enough degrees of freedom to satisfy curvature continuity requirements. In order to remedy this issue, sixth order partial differential equations were proposed by You et al. [32], Zhang and You [35], and Kubiesa et al. [17].

An important question to be answered for the PDE based approach, however, is how to solve the partial differential equations efficiently and accurately. From the properties of PEDs, one can understand that closed form solutions do not exist for the majority of surface blending problems. Numerical methods such as the finite element method [5] and finite difference method [6] are usually the most obvious choice. However, due to the nature of discretization, these reported numerical methods cannot exactly satisfy the boundary conditions of the blending problems which is a minimum requirement for surface blending. Moreover, these methods usually involve a large number of unknowns which result in the resolution of a large set of linear algebra equations. It is therefore very time-consuming. This disadvantage in many cases has significantly hampered the use of the PDE based techniques, especially in situations where interactivity is required, such as real time graphics applications. In order to create surfaces quickly, we will propose a resolution method for solving sixth order PDEs. This solution is an extension of the work presented in [34] where only a fourth order PDE was involved. This method makes use of the composite power series expansion to approximate the blending surfaces. The basic features of our method are that it can satisfy boundary conditions exactly and minimize the error of the sixth order PDEs effectively. Since only a very small number of collocation points and unknown constants are involved, the proposed method is not only accurate, but also computationally very efficient.

2. Composite power series solutions of sixth order partial differential equations

Considering the effect of the vector-valued parameters on the shape of the blending surfaces, we use the following sixth order partial differential equations to produce curvature continuous blending surfaces

$$(\mathbf{a}\frac{\partial^6}{\partial u^6}+\mathbf{b}\frac{\partial^6}{\partial u^4\partial v^2}+\mathbf{c}\frac{\partial^6}{\partial u^2\partial v^4}+\mathbf{d}\frac{\partial^6}{\partial v^6})\mathbf{x}=0 \tag{1}$$

where $\mathbf{a}=[a_x\ a_y\ a_z]^T$, $\mathbf{b}=[b_x\ b_y\ b_z]^T$, $\mathbf{c}=[c_x\ c_y\ c_z]^T$, $\mathbf{d}=[d_x\ d_y\ d_z]^T$ are vector-valued shape control parameters, $\mathbf{x}=[x\ y\ z]^T$ represents a vector-valued position function and u, v are the parametric variables.

Next, we will define the boundary conditions. According to [23], curvature continuity across the linkage curve is achieved when the second fundamental tensors of the two connected patches are identical at all points of the linkage curve. That gives,

$$(Ldu^2 + 2Mdudv + Ndv^2)_+ = (Ldu^2 + 2Mdudv + Ndv^2)_- \tag{2}$$

where subscripts "+" and "–" denote two adjacent surface patches, respectively.

Since du and dv are the differentials of two arbitrary parametric variables, Eqn (2) is equivalent to the following ones

$$L_+ = L_- \qquad M_+ = M_- \qquad N_+ = N_- \tag{3}$$

where

$$L = \mathbf{n}\mathbf{r}_{uu} \qquad M = \mathbf{n}\mathbf{r}_{uv} \qquad N = \mathbf{n}\mathbf{r}_{vv} \tag{4}$$

and

$$\begin{aligned} \mathbf{n} &= [n_1 \;\; n_2 \;\; n_3]^T \\ \mathbf{r}_{uu} &= [x_{uu} \;\; y_{uu} \;\; z_{uu}] \\ \mathbf{r}_{uv} &= [x_{uv} \;\; y_{uv} \;\; z_{uv}]^T \\ \mathbf{r}_{vv} &= [x_{vv} \;\; y_{vv} \;\; z_{vv}]^T \end{aligned} \tag{5}$$

Since the normal $\mathbf{n}$ will be shared by both surfaces, Eqn (3) will definitely be satisfied, if the following conditions hold,

$$\begin{array}{lll} (x_{uu})_+ = (x_{uu})_- & (y_{uu})_+ = (y_{uu})_- & (z_{uu})_+ = (z_{uu})_- \\ (x_{uv})_+ = (x_{uv})_- & (y_{uv})_+ = (y_{uv})_- & (z_{uv})_+ = (z_{uv})_- \\ (x_{vv})_+ = (x_{vv})_- & (y_{vv})_+ = (y_{vv})_- & (z_{vv})_+ = (z_{vv})_- \end{array} \tag{6}$$

Therefore, the boundary conditions for surface blending with up to curvature continuities will include position and tangent continuity conditions as well as Eqn (6). Thus the boundary conditions can be written as

$$\begin{array}{lllllll} for & u = 0, & \mathbf{x} = \mathbf{G}_1(v) & \mathbf{x}_u = \mathbf{G}_2(v) & \mathbf{x}_{uu} = \mathbf{G}_3(v) & \mathbf{x}_{uv} = \mathbf{G}_2'(v) & \mathbf{x}_{vv} = \mathbf{G}_1''(v) \\ for & u = 1, & \mathbf{x} = \mathbf{G}_4(v) & \mathbf{x}_u = \mathbf{G}_5(v) & \mathbf{x}_{uu} = \mathbf{G}_6(v) & \mathbf{x}_{uv} = \mathbf{G}_5'(v) & \mathbf{x}_{vv} = \mathbf{G}_4''(v) \end{array} \tag{7}$$

After the above treatment, a blending surface $\mathbf{x}(u,v)$ with curvature continuity can be created with the solution to PDE (1) subject to boundary conditions (7).

Clearly, the closed form solution of PDE (1) under boundary conditions (7) does not exist for general cases. Here we use the same methodology which we developed in [34] to find the approximate analytical solution. In order to simplify the solving process for PDE (1), we firstly define a linearly independent basic function as those consisting of constant 1, the parametric variable v, its various elementary functions excluding polynomials, and their combinations not in a polynomial form. Then, we can write the following linearly independent basic functions from the boundary conditions (7),

$$\begin{array}{lll} g_i(v) & (i = 0,\ 1,\ 2, \cdots, I) & \text{for } x \text{ componenet} \\ h_j(v) & (j = 0,\ 1,\ 2, \cdots, J) & \text{for } y \text{ componenet} \\ s_k(v) & (k = 0,\ 1,\ 2, \cdots, K) & \text{for z componenet} \end{array} \tag{8}$$

With the above preparation, we propose to approximate the blending surface, i.e. the solution of Eqn (1) subject to boundary conditions (7) with the same composite power series expansion used in [34] whose form is given by

$$\begin{aligned} x(u,v) &= \sum_{i=0}^{I} x_i(u,v) \\ &= \sum_{i=0}^{I}\sum_{m=0}^{M_{xi}} p_{im} u^m g_i(v) \\ y(u,v) &= \sum_{j=0}^{J} y_j(u,v) \\ &= \sum_{j=0}^{J}\sum_{m=0}^{M_{yj}} q_{jm} u^m h_j(v) \\ z(u,v) &= \sum_{k=0}^{K} z_k(u,v) \\ &= \sum_{k=0}^{K}\sum_{m=0}^{M_{zk}} r_{km} u^m s_k(v) \end{aligned} \tag{9}$$

where $M_{xi},\ M_{yj},\ M_{zk}$ represent the numbers of the terms of the power series taken for the $x_i,\ y_j,\ z_{\mathrm{k}}$ components, respectively.

If a linearly independent basic function of the boundary conditions (7) is 1, say for example $g_i(v) = 1$, the corresponding exponent m takes values from 0 to 5, because these 6 unknown constants can be uniquely determined by the boundary conditions given in Eqn (10).

Taking the x component as an example, referring to Eqn (9), the boundary conditions for $x_i(u,v)$ can be written as

$$\begin{aligned} &u = 0 \quad x_i = a_{i0} g_i(v) \quad \frac{\partial x_i}{\partial u} = a_{i1} g_i(v) \quad \frac{\partial^2 x_i}{\partial u^2} = a_{i2} g_i(v) \\ &\qquad \frac{\partial^2 x_i}{\partial u \partial v} = a_{i1} g_i'(v) \quad \frac{\partial^2 x_i}{\partial v^2} = a_{i0} g_i''(v) \\ &u = 1 \quad x_i = a_{i3} g_i(v) \quad \frac{\partial x_i}{\partial u} = a_{i4} g_i(v) \quad \frac{\partial^2 x_i}{\partial u^2} = a_{i5} g_i(v) \\ &\qquad \frac{\partial^2 x_i}{\partial u \partial v} = a_{i4} g_i'(v) \quad \frac{\partial^2 x_i}{\partial v^2} = a_{i3} g_i''(v) \\ &(i = 0,1,2,3,\cdots, I) \end{aligned} \tag{10}$$

Substituting $x_i(u,v)$ of Eqn (9) into Eqn (10), we find that $\frac{\partial^2 x_i}{\partial u \partial v} = a_{i1} g_i'(v)$ and $\frac{\partial x_i}{\partial u} = a_{i1} g_i(v)$ produce the same equation, and so do $\frac{\partial^2 x_i}{\partial v^2} = a_{i0} g_i''(v)$ and $x_i = a_{i0} g_i(v)$. Therefore, boundary conditions $\frac{\partial^2 x_i}{\partial u \partial v}$ and $\frac{\partial^2 x_i}{\partial v^2}$ in Eqn (10) for both $u = 0$ and $u = 1$ are redundant.

Similar to the treatment given in [34], we can now solve Eqn (10) for the unknown constants p_{im} $(m = 0, 1, 2, \cdots, 5)$. They are given by

$$
\begin{aligned}
p_{i0} &= a_{i0} \\
p_{i1} &= a_{i1} \\
p_{i2} &= 0.5a_{i2} \\
p_{i3} &= -10a_{i0} - 6a_{i1} - 1.5a_{i2} + 10a_{i3} - 4a_{i4} + 0.5a_{i5} \\
&\quad - \sum_{m=6}^{M_{xi}} (0.5m^2 - 4.5m + 10)\, p_{im} \\
p_{i4} &= 15a_{i0} + 8a_{i1} + 1.5a_{i2} - 15a_{i3} + 7a_{i4} - a_{i5} \\
&\quad + \sum_{m=6}^{M_{xi}} (m^2 - 8m + 15)\, p_{im} \\
p_{i5} &= -6a_{i0} - 3a_{i1} - 0.5a_{i2} + 6a_{i3} - 3a_{i4} + 0.5a_{i5} \\
&\quad - 0.5 \sum_{m=6}^{M_{xi}} (m^2 - 7m + 12)\, p_{im}
\end{aligned} \tag{11}
$$

Here $a_{in}\ (n = 0, 1, 2, ..., 5)$ are known constants. Replacing p_{im} ($m = 0, 1, 2, \cdots, 5$) of $x_i(u,v)$ in the first expression of Eqn (9) with Eqn (11), one obtains the following x component that satisfies boundary conditions (10) exactly

$$
\begin{aligned}
x = \sum_{i=0}^{I} \Big\{ & \left(1 - 10u^3 + 15u^4 - 6u^5\right) a_{i0} + \left(u - 6u^3 + 8u^4 - 3u^5\right) a_{i1} \\
& + 0.5\left(u^2 - 3u^3 + 3u^4 - u^5\right) a_{i2} + \left(10u^3 - 15u^4 + 6u^5\right) a_{i3} \\
& + \left(-4u^3 + 7u^4 - 3u^5\right) a_{i4} + \left(0.5u^3 - u^4 + 0.5u^5\right) a_{i5} \\
& + \sum_{m=6}^{M_{xi}} \Big[-\left(0.5m^2 - 4.5m + 10\right) u^3 + \left(m^2 - 8m + 15\right) u^4 \\
& - 0.5\left(m^2 - 7m + 12\right) u^5 + u^m \Big] p_{im} \Big\} g_i(v)
\end{aligned} \tag{12}
$$

Since Eqn (9) is an approximate solution of Eqn (1) under boundary conditions (7), Eqn (1) is not accurately satisfied by substituting Eqn (9) into (1). The error can be described with a residual function (error function). Still taking the x component as an example, its residual function can be formulated by

$$
R(u,v) = \sum_{i=0}^{I} \left(\sum_{m=6}^{M_{xi}} p_{im} U_{im} + A_i \right) \tag{13}
$$

where U_{im} and A_i can be written as

$$
\begin{aligned}
U_{im} &= m(m-1)(m-2)(m-3)(m-4)(m-5) a_x u^{m-6} g_i(v) \\
&\quad + \Big[24(m^2 - 8m + 15) - 60(m^2 - 7m + 12)u + m(m-1) \\
&\quad (m-2)(m-3)u^{m-4} \Big] b_x \frac{d^2 g_i(v)}{dv^2} + \Big[-6(0.5m^2 - 4.5m \\
&\quad + 10)u + 12(m^2 - 8m + 15)u^2 - 10(m^2 - 7m + 12)u^3 \\
&\quad + m(m-1)u^{m-2} \Big] c_x \frac{d^4 g_i(v)}{dv^4} + \Big[-(0.5m^2 - 4.5m + 10)u^3 \\
&\quad + (m^2 - 8m + 15)u^4 - 0.5(m^2 - 7m + 12)u^5 + u^m \Big] d_x \frac{d^6 g_i(v)}{dv^6}
\end{aligned} \tag{14}
$$

and

$$
\begin{aligned}
A_i = 24\Big[&(15a_{i0} + 8a_{i1} + 1.5a_{i2} - 15a_{i3} + 7a_{i4} - a_{i5}) + 5(-6a_{i0} - 3a_{i1} \\
&- 0.5a_{i2} + 6a_{i3} - 3a_{i4} + 0.5a_{i5})u\Big]b_x \frac{d^2 g_i(v)}{dv^2} + 2\Big[0.5a_{i2} + 3(-10a_{i0} \\
&- 6a_{i1} - 1.5a_{i2} + 10a_{i3} - 4a_{i4} + 0.5a_{i5})u + 6(15a_{i0} + 8a_{i1} + 1.5a_{i2} \\
&- 15a_{i3} + 7a_{i4} - a_{i5})u^2 + 10(-6a_{i0} - 3a_{i1} - 0.5a_{i2} + 6a_{i3} - 3a_{i4} \\
&+ 0.5a_{i5})u^3\Big]c_x \frac{d^4 g_i(v)}{dv^4} + \Big[a_{i0} + a_{i1}u + 0.5a_{i2}u^2 + (-10a_{i0} - 6a_{i1} \\
&- 1.5a_{i2} + 10a_{i3} - 4a_{i4} + 0.5a_{i5})u^3 + (15a_{i0} + 8a_{i1} + 1.5a_{i2} - 15a_{i3} \\
&+ 7a_{i4} - a_{i5})u^4 + (-6a_{i0} - 3a_{i1} - 0.5a_{i2} + 6a_{i3} - 3a_{i4} + 0.5a_{i5})u^5\Big] \\
&d_x \frac{d^6 g_i(v)}{dv^6}\Big\}
\end{aligned}
\tag{15}
$$

Assuming that the blending region is defined by $u_0 \le u \le u_1$ and $v_0 \le v \le v_1$, choosing N collocation points in this region and substituting the values of u and v at these collocation points into Eqn (13), the residual values $R(u_n, v_n)$ $(n = 1, 2, \cdots, N)$ at these collocation points can be computed by [30]

$$\mathbf{R} = \mathbf{AC} - \mathbf{B} \tag{16}$$

where $\mathbf{R}$, $\mathbf{C}$ and $\mathbf{B}$ are $N \times 1$ arrays consisting of the residual values, unknown constants and constant terms, respectively, and $\mathbf{A}$ is a $N \times \sum_{i=0}^{I}(M_{xi} - 5)$ matrix consisting of the coefficients of the unknown constants p_{im} $(i = 0, 1, 2, \cdots, I;\ m = 6, 7, \cdots, M_{xi})$.

The squared sum of the residual values of Eqn (16) is

$$\mathbf{I} = \mathbf{R}^T \mathbf{R} \tag{17}$$

And the blending surface minimising the error of PDE (1) can be determined by

$$\frac{\partial \mathbf{I}}{\partial \mathbf{C}} = 0 \tag{18}$$

which leads to the following set of linear algebraic equations

$$\mathbf{A}^T \mathbf{AC} = \mathbf{A}^T \mathbf{B} \tag{19}$$

Eqn (19) contains $\sum_{i=0}^{I}(M_{xi} - 5)$ unknown constants. Solving these linear algebra equations determines all the unknown constants of the x component. The y and z components can be obtained similarly.

3. Accuracy and computational efficiency

In this section we will examine the accuracy and computational efficiency of the above-proposed composite power series method through two blending examples. The first is to blend a circular torus and an elliptic hyperboloid of one sheet and the second example is to blend an open surface and a

plane. Although the first is straightforward, the second would be very challenging for other blending techniques. From this point of view, one can also sense the versatility and powerfulness of the PDE based blending approach.

It is well known that the closed form solution of a PDE is the most accurate and efficient among all possible solutions. For the first example, the closed form solution of PDE (1) under boundary conditions (20) is obtainable, if the vector-valued shape control parameters are set to those presented below. We will solve PDE (1) using both the presented method and the closed form solution method, and compare the accuracy and computational efficiency of both approaches.

The boundary conditions for this blending example are*

$$
\begin{array}{lllll}
u=0 & x = a\cosh u_0 \cos v & \dfrac{\partial x}{\partial u} = a\sinh u_0 \cos v & \dfrac{\partial^2 x}{\partial u^2} = a\cosh u_0 \cos v \\
 & y = b\cosh u_0 \sin v & \dfrac{\partial y}{\partial u} = b\sinh u_0 \sin v & \dfrac{\partial^2 y}{\partial u^2} = b\cosh u_0 \sin v \\
 & z = h_0 + h\sinh u_0 & \dfrac{\partial z}{\partial u} = h\cosh u_0 & \dfrac{\partial^2 z}{\partial u^2} = h\sinh u_0 \\
u=1 & x = (R + A\cos u_1)\cos v & \dfrac{\partial x}{\partial u} = -A\sin u_1 \cos v & \dfrac{\partial^2 x}{\partial u^2} = -A\cos u_1 \cos v \\
 & y = (R + A\cos u_1)\sin v & \dfrac{\partial y}{\partial u} = -A\sin u_1 \sin v & \dfrac{\partial^2 y}{\partial u^2} = -A\cos u_1 \sin v \\
 & z = A\sin u_1 & \dfrac{\partial z}{\partial u} = A\cos u_1 & \dfrac{\partial^2 z}{\partial u^2} = -A\sin u_1
\end{array}
\tag{20}
$$

From the boundary conditions, it can be seen that the linearly independent basic functions are $\cos v$ for the x component, $\sin v$ for the y component and 1 for the z component. Therefore, the solution of Eqn (1) takes the form of

$$
\begin{aligned}
x &= \sum_{m=0}^{M_{x0}} p_{0m} u^m \cos v \\
y &= \sum_{m=0}^{M_{y0}} q_{0m} u^m \sin v \\
z &= \sum_{m=0}^{5} r_{0m} u^m
\end{aligned}
\tag{21}
$$

Using the method introduced in the previous section, we can determine all the unknown constants of Eqn (21). Let us evenly distribute 9 collocation points within the rectangular region of u and v, and take the numbers of the power series terms of the x and y components to be $M_{x0} = M_{y0} = 7$. This means that there are only 2 unknown constants in the solving equation (19) to be determined. When setting the vector-valued parameters to be $a_x = b_x = a_y = b_y = 1$ and $c_x = d_x = c_y = d_y = -1$, the blending surface is obtained and depicted in Fig. 1a.

* Undefined symbols used in the examples throughout this paper are geometric parameters of the relevant example.

Substituting the same vector-valued shape control parameters into PDE (1), the sixth order partial differential equations for the x and y components of Eqn (1) become

$$\left(\frac{\partial^6}{\partial u^6}+\frac{\partial^6}{\partial u^4\partial v^2}-\frac{\partial^6}{\partial u^2\partial v^4}-\frac{\partial^6}{\partial v^6}\right)\begin{pmatrix}x\\y\end{pmatrix}=0 \tag{22}$$

Under the same boundary conditions, the closed form solution of Eqn (22) exists which has the following form

$$\begin{aligned} x &= f(u)\cos v \\ y &= g(u)\sin v \end{aligned} \tag{23}$$

It should be pointed out that the closed form solutions of Eqn (1) under the same boundary conditions for arbitrary values of the vector-valued parameters are usually not obtainable.

Introducing Eqn (23) into (22), we can obtain x and y components. The z component can be taken to be the third of Eqn (21) which satisfies the sixth order PDE of the z component. Therefore the closed form solution of Eqn (1) is

$$\begin{aligned} x &= \left[(c_1+c_2u)e^u+(c_3+c_4u)e^{-u}+c_5\cos u+c_6\sin u\right]\cos v \\ y &= \left[(d_1+d_2u)e^u+(d_3+d_4u)e^{-u}+d_5\cos u+d_6\sin u\right]\sin v \\ z &= r_{00}+r_{01}u+r_{02}u^2+r_{03}u^3+r_{04}u^4+r_{05}u^5 \end{aligned} \tag{24}$$

where all the unknown constants can be determined by the boundary conditions of this blending problems.

With Eqn (24), we generated the blending surface and depicted it in Fig. 1b. Visually, the images shown in both figures look identical.

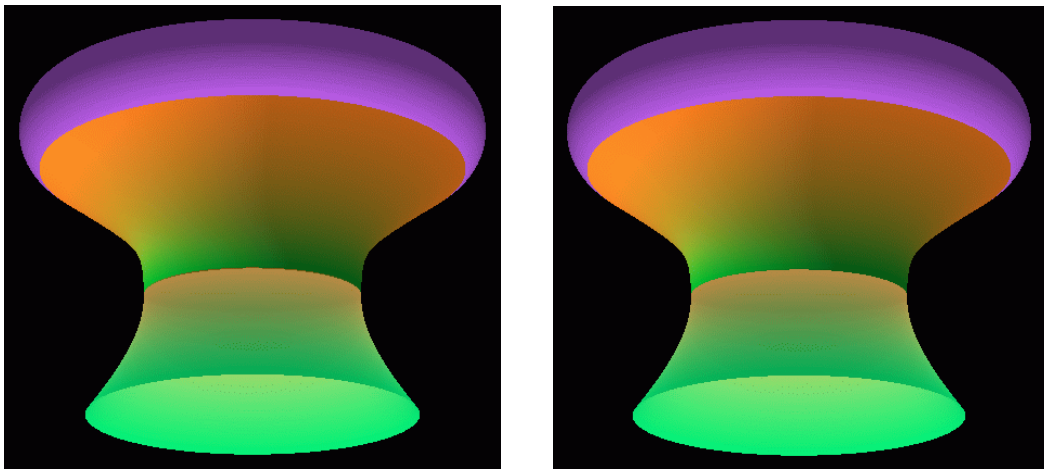

a b

Fig. 1. Blending between a circular torus and an elliptic hyperboloid of one sheet

Excellent agreement of the blending surfaces between the proposed composite power series method and closed form solution can be further demonstrated through a quantitative comparison. We use the Euclidean norm to measure the difference. Choosing I_u and J_v points respectively in the x and y directions within the blending region, the Euclidean norm can be written as

$$E = \left\{ \frac{1}{I_u \times J_v} \sum_{i=1}^{I_u} \sum_{j=1}^{J_v} \left\{ \left[x(u_i, v_j) - \tilde{x}(u_i, v_j) \right]^2 + \left[y(u_i, v_j) - \tilde{y}(u_i, v_j) \right]^2 + \left[z(u_i, v_j) - \tilde{z}(u_i, v_j) \right]^2 \right\}^{\frac{1}{2}} \right\} \tag{25}$$

where the x, y and z components without "~" stand for the closed form solutions and those with "~" for the composite power series solutions.

Equation (25) is a measurement of the absolute errors between two surfaces. We can also use relative errors between two surfaces to measure the difference between the proposed composite power series solution and the closed form solution. The equation of the relative errors takes the form of

$$\overline{E} = \frac{1}{I_u \times J_v} \sum_{i=1}^{I_u} \sum_{j=1}^{J_v} \left\{ \left\{ \left[x(u_i, v_j) - \tilde{x}(u_i, v_j) \right]^2 + \left[y(u_i, v_j) - \tilde{y}(u_i, v_j) \right]^2 + \left[z(u_i, v_j) - \tilde{z}(u_i, v_j) \right]^2 \right\}^{\frac{1}{2}} \Big/ \left\{ \left[x(u_i, v_j) \right]^2 + \left[y(u_i, v_j) \right]^2 + \left[z(u_i, v_j) \right]^2 \right\}^{\frac{1}{2}} \right\} \tag{26}$$

Uniformly choosing 99×99 points within the blending region, i.e., $I_u = J_v = 99$, the Euclidean norm between these two blending surfaces is only $E = 6.111 \times 10^{-3}$ and the difference from Eqn (26) is $\overline{E} = 3.135 \times 10^{-3}$. It suggests that with even a small number of collocation points and power series terms, the proposed composite power series method can generate blending surfaces almost as accurately as the closed form solution method. Considering how the method works, the reason is easy to comprehend: since the proposed composite power series method always satisfies the boundary conditions exactly up to the order of curvature continuity, the discrepancy at the interior region of the blending surface will have very limited effect both visually and functionally. Moreover, this discrepancy is further reduced by the least square minimisation, leaving almost no room for errors.

It is also worthy mentioning that the computing efficiency of the proposed method is much higher than that of the other numerical methods such as the finite element method and the finite difference method. The finite element method, for example, uses a large number of elements or nodes to achieve reasonable accuracy, which involves with many unknowns. As a consequence, the resolution of the linear equations is inevitably time-consuming. The proposed method on the other hand, only needs to solve a small number of linear equations. With the above-chosen number of the collocation points and power series terms, the resolution process took less than 10^{-6} second for the proposed composite power series and closed form resolution methods on an ordinary PC. This is also true even if we chose $8 \times 8 = 64$ collocation points and $M_{x0} = M_{y0} = 9$ power series terms. Thus we can conclude that the proposed composite power series method can generate blending surfaces almost as accurately and fast as the closed form solution method. The computational efficiency is the same also for the problems whose closed form solutions do not exist, thus making many previously unsolvable problems solvable.

For the second example, the boundary conditions are given by

$$
\begin{array}{lll}
u=0 \quad x=0.1\sinh(0.1v+0.1)+1.1088\sin v & \dfrac{\partial x}{\partial u}=-0.132\sin v & \dfrac{\partial^2 x}{\partial u^2}=1.32\sin v \\
\quad\quad y=0.9\cosh 0.3v+1.1088\cos v & \dfrac{\partial y}{\partial u}=-0.132\cos v & \dfrac{\partial^2 y}{\partial u^2}=1.32\cos v \\
\quad\quad z=0.5+e^{0.2} & \dfrac{\partial z}{\partial u}=-e^{0.2} & \dfrac{\partial^2 z}{\partial u^2}=e^{0.2} \\
u=1 \quad x=1.6\sin v & \dfrac{\partial x}{\partial u}=1.6\sin v & \dfrac{\partial^2 x}{\partial u^2}=0 \\
\quad\quad y=1.6\cos v & \dfrac{\partial y}{\partial u}=1.6\cos v & \dfrac{\partial^2 y}{\partial u^2}=0 \\
\quad\quad z=0.8 & \dfrac{\partial z}{\partial u}=0 & \dfrac{\partial^2 z}{\partial u^2}=0
\end{array}
\tag{27}
$$

The vector-valued parameters in Eqn (1) were taken to be $a_i=1$, $b_i=3p^2$, $c_i=3p^4$, $d_i=p^6$ $(i=x,y,z)$ and $p=3$. The image obtained from the proposed composite power series and closed form solutions were depicted in Figs. 2a and 2b, respectively. Again both methods produced identical images.

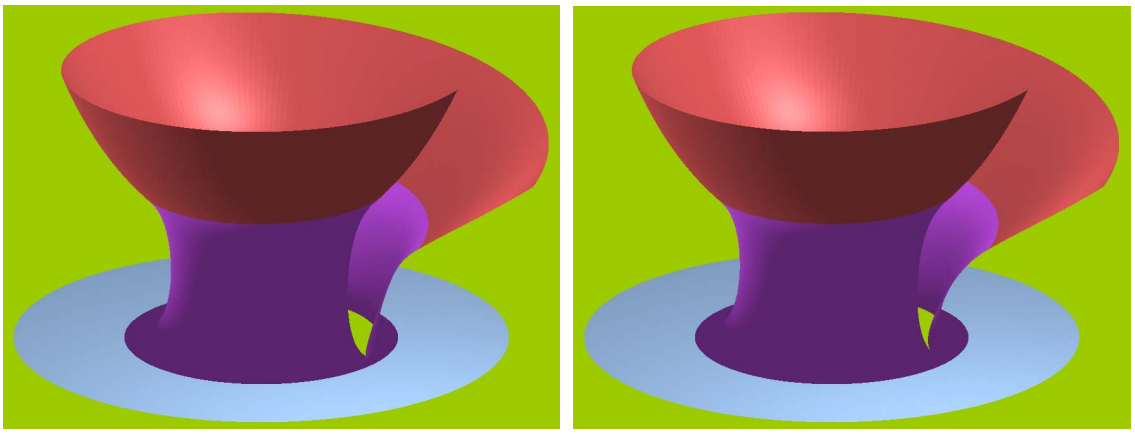

a b

Fig. 2. Blending between an open surface and a plane

4. Influences of vector-valued shape control parameters on surface shapes

By using different values of the vector-valued shape control parameters, the solution to PDE (1) is changed which will lead to different surface shapes. In this section, we will use two examples to highlight their effects.

The first example is to blend a sphere and an ellipsoid. The boundary conditions for this blending task are given below

$$
\begin{array}{lllll}
u=0 & x=\dfrac{\sqrt{3}}{2}r\cos v & \dfrac{\partial x}{\partial u}=-\dfrac{1}{2}r\cos v & \dfrac{\partial^2 x}{\partial u^2}=-\dfrac{\sqrt{3}}{2}r\cos v \\
 & y=\dfrac{\sqrt{3}}{2}r\sin v & \dfrac{\partial y}{\partial u}=-\dfrac{1}{2}r\sin v & \dfrac{\partial^2 y}{\partial u^2}=-\dfrac{\sqrt{3}}{2}r\sin v \\
 & z=\dfrac{1}{2}r & \dfrac{\partial z}{\partial u}=\dfrac{\sqrt{3}}{2}r & \dfrac{\partial^2 z}{\partial u^2}=-\dfrac{1}{2}r \\
u=1 & x=\dfrac{\sqrt{3}}{2}a\cos v & \dfrac{\partial x}{\partial u}=-\dfrac{1}{2}a\cos v & \dfrac{\partial^2 x}{\partial u^2}=-\dfrac{\sqrt{3}}{2}a\cos v \\
 & y=\dfrac{\sqrt{3}}{2}b\sin v & \dfrac{\partial y}{\partial u}=-\dfrac{1}{2}b\sin v & \dfrac{\partial^2 y}{\partial u^2}=-\dfrac{\sqrt{3}}{2}b\sin v \\
 & z=\dfrac{1}{2}c & \dfrac{\partial z}{\partial u}=\dfrac{\sqrt{3}}{2}c & \dfrac{\partial^2 z}{\partial u^2}=-\dfrac{1}{2}c
\end{array}
\tag{28}
$$

The solution of Eqn (1) under these boundary conditions has the same form as that of Eqn (21). We will take 3×3 collocation points and 2 unknown constants. Initially, we set the vector-valued parameters to $a_x=b_x=c_x=d_x=a_y=b_y=c_y=d_y=1$. The obtained blending surface is depicted in Fig. 3a. Then making $c_x=c_y=10^4$ and keeping all other parameters unchanged, we obtain the blending surface in Fig. 3b.

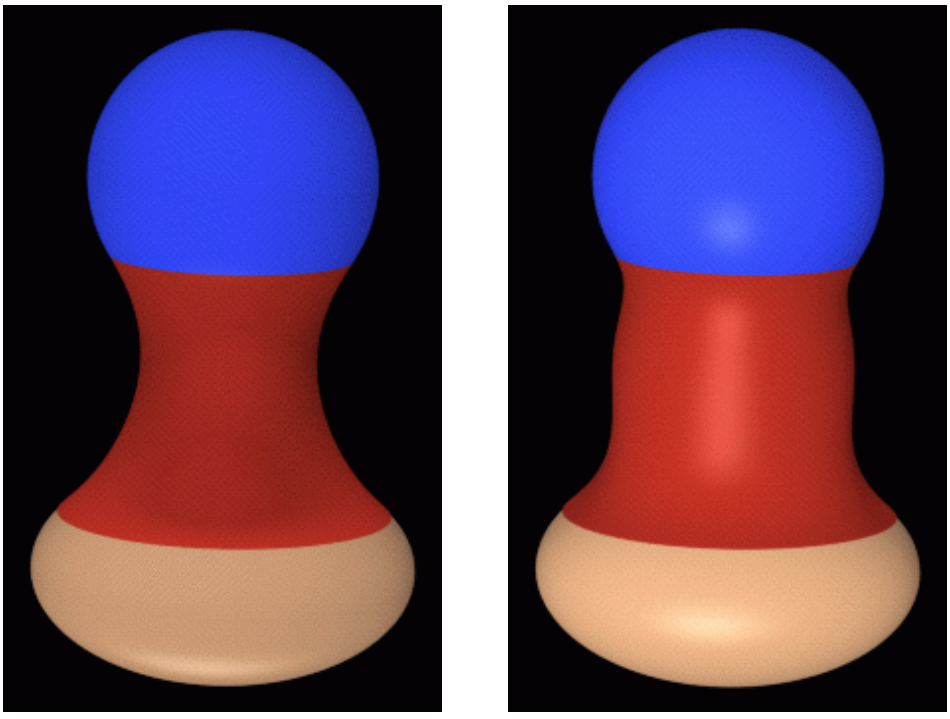

a b

Fig. 3. Blending between a sphere and an ellipsoid

The second example is to blend a conical frustum with an elliptic cylinder. The boundary conditions for this blending task are taken as

$$
\begin{array}{llll}
u=0 & x=ru_0^2\cos v & \dfrac{\partial x}{\partial u}=2ru_0\cos v & \dfrac{\partial^2 x}{\partial u^2}=2r\cos v \\
 & y=ru_0 v\sin v & \dfrac{\partial y}{\partial u}=rv\sin v & \dfrac{\partial^2 y}{\partial u^2}=0 \\
 & z=hu_0 & \dfrac{\partial z}{\partial u}=h & \dfrac{\partial^2 z}{\partial u^2}=0 \\
u=1 & x=x_0+a\cos\alpha\cos v+h_1u_1\sin\alpha & \dfrac{\partial x}{\partial u}=h_1\sin\alpha & \dfrac{\partial^2 x}{\partial u^2}=0 \\
 & y=b\sin v & \dfrac{\partial y}{\partial u}=0 & \dfrac{\partial^2 y}{\partial u^2}=0 \\
 & z=z_0-a\sin\alpha\cos v+h_1u_1\cos\alpha & \dfrac{\partial z}{\partial u}=h_1\cos\alpha & \dfrac{\partial^2 z}{\partial u^2}=0
\end{array}
\tag{29}
$$

Using the above described procedure, the solution of Eqn (1) under these boundary conditions takes the form of

$$
\begin{aligned}
x &= \sum_{m=0}^{5} p_{0m}u^m + \sum_{m=0}^{M_{x1}} p_{1m}u^m\cos v \\
y &= \sum_{m=0}^{M_{y0}} q_{0m}u^m v\sin v + \sum_{m=0}^{M_{y1}} q_{1m}u^m\sin v \\
z &= \sum_{m=0}^{5} r_{0m}u^m + \sum_{m=0}^{M_{z1}} r_{1m}u^m\cos v
\end{aligned}
\tag{30}
$$

Using the proposed method, the unknown constants of Eqn (30) can be similarly determined. With the collocation points and the unknown constants unchanged, the blending surface in Fig. 4a is obtained when all the vector-valued parameters are set to 1, and Fig. 4b created when parameters b_x, b_y and b_z are set to 100 and the others are kept the same.

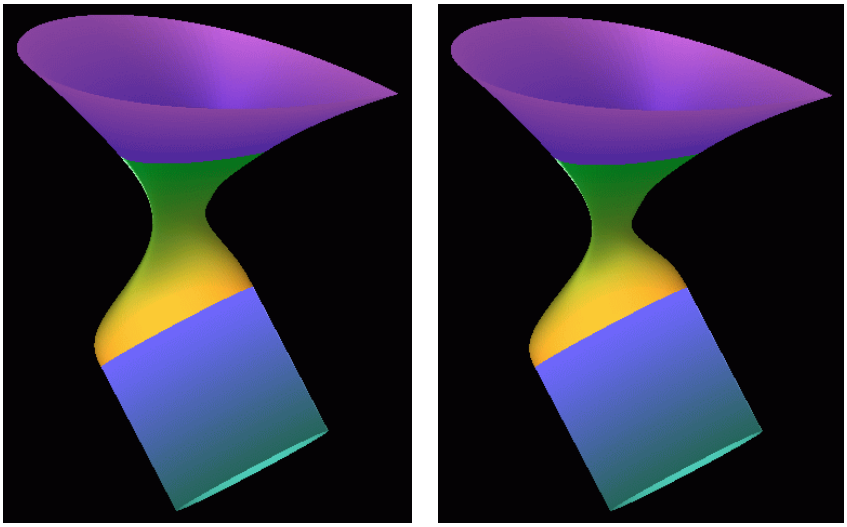

a b

Fig. 4. Blending between a conical frustum and an elliptic cylinder

It is evident that the vector-valued shape control parameters in Eqn (1) have a strong influence on the shape of the blending surfaces. By changing their values, we can generate different surface shapes.

5. More complex examples

Two more complex examples of surface blending will be presented to demonstrate the strength of the proposed approach. The first is to blend two intersecting cylinders, whose PDE was solved only with the finite element method or finite difference method in existing literature, which is numerically expensive. The second example is to determine the transition surface between an open surface and a plane interpolating a specified curve.

For the blending between two intersecting cylinders, the boundary conditions at the linkage curves are as follows

$$
\begin{array}{llll}
u=0 & x=s\cos v & \dfrac{\partial x}{\partial u}=0 & \dfrac{\partial^2 x}{\partial u^2}=0 \\
 & y=s\sin v & \dfrac{\partial y}{\partial u}=0 & \dfrac{\partial^2 y}{\partial u^2}=0 \\
 & z=\sqrt{(r+k_1)^2-s^2\cos^2 v} & \dfrac{\partial z}{\partial u}=\dfrac{r+k_1}{\sqrt{(r+k_1)^2-s^2\cos^2 v}} & \dfrac{\partial^2 z}{\partial u^2}=\dfrac{1}{\sqrt{(r+k_1)^2-s^2\cos^2 v}} \\
 & & & -\dfrac{(r+k_1)^2}{\sqrt[3]{(r+k_1)^2-s^2\cos^2 v}} \\
u=1 & x=(s+l_1)\cos v & \dfrac{\partial x}{\partial u}=\cos v & \dfrac{\partial^2 x}{\partial u^2}=0 \\
 & y=(s+l_1)\sin v & \dfrac{\partial y}{\partial u}=\sin v & \dfrac{\partial^2 y}{\partial u^2}=0 \\
 & z=\sqrt{r^2-(s+l_1)^2\cos^2 v} & \dfrac{\partial z}{\partial u}=\dfrac{(s+l_1)\cos^2 v}{\sqrt{r^2-(s+l_1)^2\cos^2 v}} & \dfrac{\partial^2 z}{\partial u^2}=\dfrac{\cos^2 v}{\sqrt{r^2-(s+l_1)^2\cos^2 v}} \\
 & & & -\dfrac{(s+l_1)^2\cos^4 v}{\sqrt[3]{r^2-(s+l_1)^2\cos^2 v}}
\end{array}
\tag{31}
$$

According to these boundary conditions, we can obtain the linearly independent basic functions and construct the following composite power series solution of Eqn (1)

$$
\begin{aligned}
x &= \sum_{m=0}^{M_{x0}} p_{0m} u^m \cos v \\
y &= \sum_{m=0}^{M_{y0}} q_{0m} u^m \sin v \\
z &= \sum_{m=0}^{M_{z0}} r_{0m} u^m \sqrt{(r+k_1)^2 - s^2 \cos^2 v} + \sum_{m=0}^{M_{z1}} \frac{r_{1m} u^m}{\sqrt{(r+k_1)^2 - s^2 \cos^2 v}} \\
&+ \sum_{m=0}^{M_{z2}} \frac{r_{2m} u^m}{\sqrt[3]{(r+k_1)^2 - s^2 \cos^2 v}} + \sum_{m=0}^{M_{z3}} r_{3m} u^m \sqrt{r^2 - (s+l_1)^2 \cos^2 v} \\
&+ \sum_{m=0}^{M_{z4}} \frac{r_{4m} u^m \cos^2 v}{\sqrt{r^2 - (s+l_1)^2 \cos^2 v}} + \sum_{m=0}^{M_{z5}} \frac{r_{5m} u^m \cos^4 v}{\sqrt[3]{r^2 - (s+l_1)^2 \cos^2 v}}
\end{aligned}
\tag{32}
$$

On determining the unknown constants of the above equation, the blending surface generated is depicted in Fig. 5.

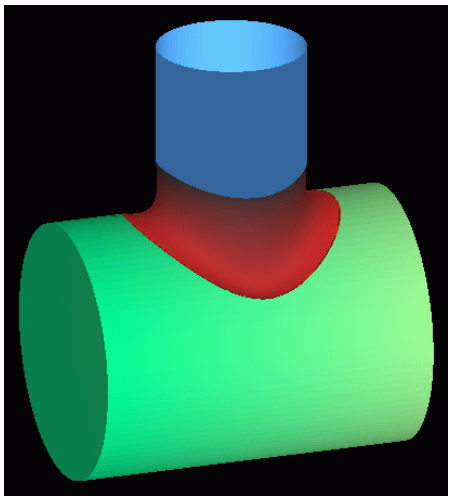

Fig. 5. Blending between two intersecting cylinders

For the blending between an open surface and a plane at a specified curve, the parametric equation of the open surface are taken to be

$$
\begin{aligned}
x &= a_1 \sinh(a_2 v + a_3) + a_4 (1 + u^3) \sin a_5 v \\
y &= b_1 \cosh b_2 v + b_3 (1 + u^3) \cos b_4 v \\
z &= c_1 + c_2 e^u
\end{aligned}
\tag{33}
$$

Taking $u = 0.2$ in the above equation and specifying the curve on the plane to be blended, we can obtain the boundary conditions of this blending task

$$
\begin{array}{llll}
u=0 & x=a_1\sinh(a_2v+a_3)+1.008a_4\sin a_5v & \dfrac{\partial x}{\partial u}=a_4'\sin a_5v & \dfrac{\partial^2 x}{\partial u^2}=1.2a_4\sin a_5v \\
 & y=b_1\cosh b_2v+1.008b_3\cos b_4v & \dfrac{\partial y}{\partial u}=b_3'\cos b_4v & \dfrac{\partial^2 y}{\partial u^2}=1.2b_3\cos b_4v \\
 & z=c_1+c_2e^{0.2} & \dfrac{\partial z}{\partial u}=c_2e^{0.2} & \dfrac{\partial^2 z}{\partial u^2}=c_2e^{0.2} \\
u=1 & x=a_6\sin a_7v+a_8\sin a_9v & \dfrac{\partial x}{\partial u}=a_6'\sin a_7v & \dfrac{\partial^2 x}{\partial u^2}=0 \\
 & y=b_5\cos b_6v+b_7\cos b_8v & \dfrac{\partial y}{\partial u}=b_5'\cos b_6v & \dfrac{\partial^2 y}{\partial u^2}=0 \\
 & z=c_3 & \dfrac{\partial z}{\partial u}=0 & \dfrac{\partial^2 z}{\partial u^2}=0
\end{array}
\tag{34}
$$

The composite power series solution of Eqn (1) corresponding to the linearly independent basic functions in these boundary conditions can be taken to have the following form

$$
\begin{aligned}
x &= \sum_{m=0}^{M_{x0}} p_{0m}u^m\sinh(a_2v+a_3)+\sum_{m=0}^{M_{x1}} p_{1m}u^m\sin a_5v+\sum_{m=0}^{M_{x2}} p_{2m}u^m\sin a_7v+\sum_{m=0}^{M_{x3}} p_{3m}u^m\sin a_9v \\
y &= \sum_{m=0}^{M_{y0}} q_{0m}u^m\cosh b_2v+\sum_{m=0}^{M_{y1}} q_{1m}u^m\cos b_4v+\sum_{m=0}^{M_{y2}} q_{2m}u^m\cos b_6v+\sum_{m=0}^{M_{y3}} q_{3m}u^m\cos b_8v \\
z &= \sum_{m=0}^{5} r_{0m}u^m
\end{aligned}
\tag{35}
$$

Specifying the values of all the geometric parameters in the boundary conditions and then determining all the unknown constants in Eqn (35) with the above proposed method, the blending surface obtained is given in Fig. 6.

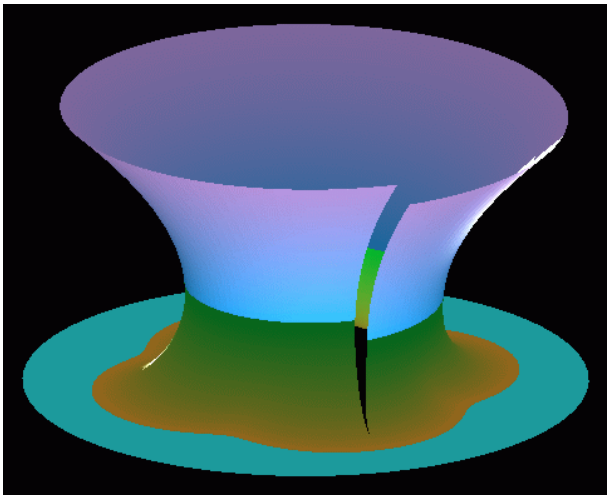

Fig. 6. Blending between an open surface and a plane at a specified curve

6. Conclusions

By solving sixth order partial differential equations with four vector-valued shape control parameters subject to blending boundary conditions, we have presented a method for surface blending with up to curvature continuities. In comparison with our previous work [34], we are able to solve a higher order (sixth order) PDE as efficiently as a lower order one, and offer better smoothness.

Traditionally, PDE based methods are only applicable to a limited number of applications. This is due to the fact that the closed form solution of a PDE is either extremely difficult to obtain or does not exist. Existing numerical methods are computationally expensive. This is rather regrettable, as such methods do offer many advantages over other surface blending approaches. In order to overcome this limitation and make our proposed PDE approach practicable to a large number of blending problems, we have developed an efficient and accurate resolution method using the composite power series expansion and the weighted residual technique. This method can satisfy the boundary conditions exactly and minimise the errors at the interior region of the surface. With this method, the generated blending surface shares the exact position, tangent and curvature values with the primary surfaces at the linkage curves. It was found that this method has almost the same accuracy and computational efficiency as the closed form solutions.

The influences of the vector-valued shape control parameters on the shape of the blending surfaces have also been examined. Their variations have a strong influence on the shape of the generated blending surfaces, and thus can be potentially exploited to serve as user interface tools for shape manipulation.

References

1. Aumann, G. (1995), Curvature continuous connections of cones and cylinders, Computer Aided Geometric Design 27(4), 293-301.
2. Bloor, M. I. G. and Wilson, M. J. (1990), Using Partial differential equations to generate free-form surfaces, Computer-Aided Design 22(4), 202-212.
3. Boehm, W. (1986), curvature continuous curves and surfaces, Computer Aided Design 18(2), 105-106.
4. Bohl, H. and Reif, U. (1997), Degenerate Bézier patches with continuous curvature, Computer Aided Geometric Design 14(8), 749-761.
5. Brown, J. M., Bloor, M. I. G., Bloor, M. S. and Wilson, M. J. (1998), The accuracy of B-spline finite element approximations to PDE surfaces, Computer Methods in Applied Mechanics and Engineering 158(3-4), 221-234.

6. Cheng, S. Y., Bloor, M. I. G., Saia, A. and Wilson, M. J. (1990), Blending between quadric surfaces using partial differential equations. In Ravani B (ed): Advances in Design Automation, Vol. 1, Computer Aided and Computational Design. ASME, 257-263.
7. Dekanski, C. W., Bloor, M. I. G. and Wilson, M. J. (1995), The generation of propeller blade geometries using the PDE method, Journal of Ship Research 39(2), 108-116.
8. Du, H. and Qin, H. (2000), Direct manipulation and interactive sculpting of PDE surfaces, Computer Graphics Forum 19(3), 261-270.
9. Du, H. and Qin, H. (2005), Dynamic PDE-based surface design using geometric and physical constraints, Graphical Models 67(1), 43-71.
10. Farin, G. (1989), Curvature continuity and offsets for piecewise conics, ACM Transactions on Graphics 8(2), 89-99.
11. Filkins P. C., Tuohy S. T. and Patrikalakis N. M. (1993), Computational methods for blending surface approximation, Engineering with Computers 9(1), 49-62.
12. Hartmann, E. (1995), blending an implicit with a parametric surface, Computer Aided Geometric Design 12(8), 825-835.
13. Hartmann, E. (1996), G^2 interpolation and blending on surfaces, The Visual Computer 12(4), 181-192.
14. Hartmann, E. (2001), Implicit G^n-blending of vertices, Computer Aided Geometric Design 18(3), 267-285.
15. Jones, A. K. (1988), Nonrectangular surface patches with curvature continuity, Computer Aided Design 20(6), 325-335.
16. Kim, H., Oh, S., Yim, J.-W. (2005), Smooth surface extension with curvature bound, Computer Aided Geometric Design 22(1), 27-43.
17. Kubiesa, S., Ugail, H. and Wilson, M. J. (2004), Interactive design using higher order PDEs, Visual Computer 20(10), 682-693.
18. Lowe, T.W., Bloor, M. I. G. and Wilson, M. J. (1990), Functionality in blend design, Computer Aided Design 22(10), 655-665.
19. Mimis, A. P., Bloor, M. I. G. and Wilson, M. J. (2001), Shape parameterization and optimization of a two-stroke engine, Journal of Propulsion and Power 17(3), 492-498.
20. Monterde, J. and Ugail, H. (2006), A general 4th-order PDE method to generate Bézier surfaces from the boundary, Computer Aided Geometric Design 23(2), 208-225.
21. Pegna, J. (1989), Simple practical criterion to guarantee second order smoothness of blend surfaces, Computer-Aided and Computational Design 19(1), 93-105.
22. Pegna, J. (1990), Spherical and circular blending of functional surfaces, Journal of Offshore Mechanics and Arctic Engineering 112(2), 134-142.
23. Pegna, J. and Wolter, F.-E. (1992), Geometrical criteria to guarantee curvature continuity of blend surfaces, Journal of Mechanical Design, Transactions of the ASME 114, 201-210.

24. Peters, J. (1996), Curvature continuous spline surfaces over irregular meshes, Computer Aided Geometric Design 13(2), 101-131.
25. Schichtel, M. (1993), G^2 Blend surfaces and filling of N-sided holes, IEEE Computer Graphics & Applications 13(5), 68-73.
26. Ugail, H. and Wilson, M. J. (2003), Efficient shape parametrisation for automatic design optimisation using a partial differential equation formulation, Computers and Structures 81(28-29), 2601-2609.
27. Ye, X. Z. (1996), The Gaussian and mean curvature criteria for curvature continuity between surfaces, Computer Aided geometric Design 13(6), 549-567.
28. Ye, X. Z. (1997), Curvature continuous interpolation of curve meshes, Computer Aided Geometric Design 14(2), 169-190.
29. You L. H. and Zhang, J. J. (1999), Blending surface generation with a fourth order partial differential equation, The Sixth International Conference on Computer-Aided Design and Computer Graphics, Shanghai, China, 1035-1039.
30. You, L. H., Zhang, J. J. and Comninos, P. (2000), A volumetric deformable muscle model for computer animation using weighted residual method, Computer Methods in Applied Mechanics and Engineering 190, 853-863.
31. You, L. H. and Zhang J. J. (2003), Fast Generation of 3D Deformable Moving Surfaces, IEEE Transactions on Systems, Man and Cybernetics, Part B: Cybernetics 33(4), 616-625.
32. You, L. H., Comninos, P. and Zhang, J. J. (2004), PDE blending surfaces with C^2 continuity, Computers & Graphics 28, 895-906.
33. Zhang, J. J. and You, L. H. (2002), PDE based surface representation-Vase design, Computers & Graphics 26, 89-98.
34. Zhang, J. J. and You, L. H. (2004), Surface blending using a power series solution to fourth order partial differential equations, International Journal of Shape Modeling 10(2), 155-185.
35. Zhang J. J. and You, L. H. (2004), Fast Surface Modelling Using a 6th Order PDE, Computer Graphics Forum 23(3), 311-320.
36. Zheng, J. M., Wang, G. Z. and Liang, Y. D. (1992), Curvature continuity between adjacent rational Bézier patches, Computer Aided Geometric Design 9(5), 321-335.